IEEE Access
Multidisciplinary | Rapid Review | Open Access Journal

Received January 8, 2020, accepted February 6, 2020, date of publication February 10, 2020, date of current version February 19, 2020.

Digital Object Identifier 10.1109/ACCESS.2020.2972967

A New Method to Evaluate Yarn Appearance Qualities Based on Machine Vision and Image Processing

ZHISONG LI, PING ZHONG, XIN TANG, YU CHEN, SHU SU, AND TIANBAO ZHAI
Donghua University, Shanghai 201620, China

Corresponding author: Ping Zhong (pzhong937@dhu.edu.cn)

This work was supported in part by the National Natural Science Foundation of China under Grant 51975116, in part by the Fundamental Research Funds for the Central Universities, and in part by the Graduate Student Innovation Fund of Donghua University under Grant GUSF-DH-D-2019088.

ABSTRACT For improving the efficiency, flexibility and robustness of yarn defect system, a new method is proposed to evaluate the quality of yarn by testing the yarn diameter, defects and hairiness based on machine vision and image processing technology. Firstly, the diameter image processing unit (DIPU) is defined and a series of sampling points are selected from moving yarn, and the DIPU corresponding to each sampling point is segmented from the captured yarn images. The average diameter of DIPU is used to represent the yarn diameter of the test points. In the extraction of yarn images, the DIPU is divided into definite foreground region, definite background region and unknown region according to the characteristics of gray-level projection distribution, and the unknown region is further processed with Poisson matting method, in which the yarn image and background image are completely separated by a defined connectivity classifier. After the yarn core is extracted by the classifier, the hairiness is divided by using image subtraction. Finally, in order to further evaluate the quality of yarn, the yarn defects were analyzed by the method of statistical methods.

INDEX TERMS Yarn quality evaluation, diameter image processing unit (DIPU), Poisson matting, connectivity classifier, hairiness extraction, yarn defects statistics.

I. INTRODUCTION

The yarn diameter, hairiness rate and defects are not only the main parameters for fabric structure but also the main performance index to evaluate the quality of yarn. In textile manufacture, the yarn diameter plays a very important role in winding, warping, weaving, knitting and sewing. It can also influence the looks, surface characteristics, handle and comfort, and other important properties [1]–[3]. Moreover, the performance of yarn will directly affect the fabric price, classification, strength utilization coefficient, etc [4]. Therefore, finding a way to get the determination of yarn diameter accurately and rapidly is a meaningful work in textile industry. With the rapid development of textile fiber materials, more and more new types of yarn such as textured yarn and blended yarn have come to our sight [5], [6]. At present, there is a great difference among the actual diameter coefficients for staple yarns. This requires new methods to measure yarn diameter accurately and efficiently. But considering the inherent characteristic of textile materials, the cross-section in different positions along the axis of the yarn is easy to change. It is a pretty heavy work to conduct a large number of sample statistics. Although the optical detection method can achieve high precision measurement [7], [8], the difficulties in identifying yarn core and hairiness make it difficult to work [9], [10].

At present, there are four main methods for yarn diameter measurement. The first method is the test of capacitance evenness, in which the air capacitor is used as a sensing element [11]. When a piece of yarn is delivered between the two metal plates where an electric field exists, the capacitance will be changed with the amount of fiber. This method could not be affected by the shape and position of yarn cross-section, and the evenness index of yarn can be easily obtained. However, the unevenness of yarn moisture and blending ratio will make the results unreliable [12], [13]. The second method is photoelectric measurement [14], [15]. Through projecting laser beam on the surface of yarn and analyzing the

The associate editor coordinating the review of this manuscript and approving it for publication was Manuel Rosa-Zurera.

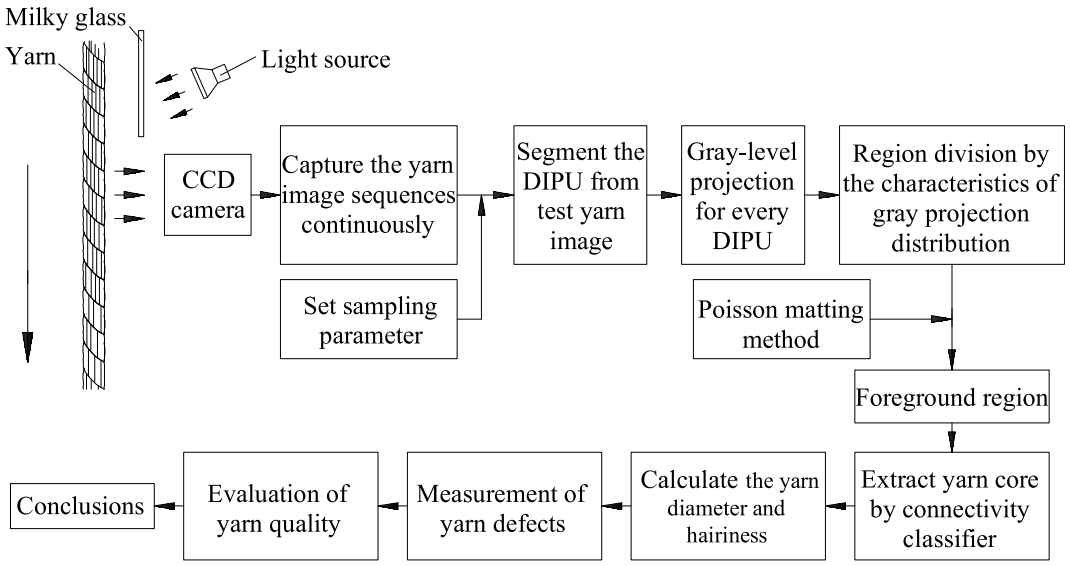

FIGURE 1. Flowchart of the method to detect yarn parameters and evaluate yarn quality.

projection images captured from image sensor, the diameter can be obtained. Although this method is not affected by the moisture and blending ratio of the yarn, the hairiness and tension can easily lead to error in the results [16], [17]. The third approach is the biological microscope, in which the yarn diameter is measured by proofreading the objective micrometer using a biological microscope. Obviously, manual operation will reduce the measuring efficiency, so this method is only suitable for scientific research in the laboratory. With the fast development of computer science and high resolution image sensors, machine vision is widely used in various detection fields and plays a more and more critical role. Many literatures have reported the use of machine vision to detect yarn diameter [11], [18]–[20]. These methods are characterized by high reliability and efficiency [21], [22], and can resolve many complex problems which are resolved difficultly with the traditional methods [23], [24]. However, in the current visual detection system, there are still many challenges, such as how to improve detection efficiency which is helpful to realize real-time detection [25], [26], how to analyze the uncertainty of yarn diameter caused by yarn shape change and ensure the accuracy of hairiness detection [27], [28].

In this paper, a new method and corresponding detection system are proposed and designed to analyze the yarn characteristics flexibly, efficiently and reliably. Based on this method, the sequential sampling points from the captured yarn images are selected. Once the operation begins, the yarn image sequences are captured continuously, and then the relevant parameters of yarn can be obtained without manual intervention. The proposed method can be used to measure and analyze the yarn diameter, hairiness and defects. And the experiments on many yarn samples demonstrate that our method can achieve good measurement accuracy.

II. METHOD TO DETECT YARN PARAMETERS

This section shows the method to detect yarn diameter, hairiness and defects based on machine vision and image processing. The flowchart of the proposed method is shown in Fig.1. And the corresponding algorithms are described in the following.

A. DIAMETER IMAGE PROCESSING UNIT (DIPU)

Due to the variability of external conditions and environment, the yarn stress from different positions in the longitudinal and transverse directions is easy to change during testing, which easily leads to irregular shape in different positions. In addition, the hairiness is randomly distributed around the yarn core. All of these factors will bring about the instability of the test result. In order to reduce the impact of random factors on the measurement, an approach to determine the diameter of yarn location points by using a diameter image processing unit (DIPU) was proposed. The average diameter of all the pixel points from the axis line with the range of 2δ is taken as the diameter of the test points. Here δ is selected by the requirements for sample detection and the compute power. In this paper, the value of δ is usually 2$\sim$8mm. While the test yarn passes through the imaging region at a certain speed, the image sequences are captured by CCD imaging system and the DIPUs can be obtained according to user setting parameters.

B. PREPROCESSING FOR DIPU

In order to improve the measurement accuracy of the yarn diameter, image preprocessing is used to improve the image

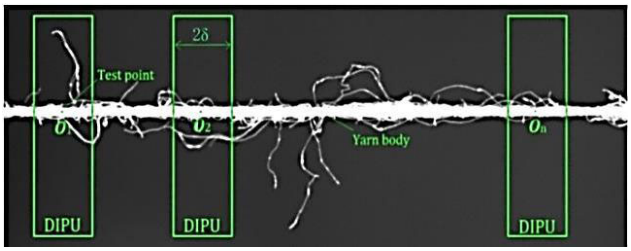

FIGURE 2. Selection method of the diameter image processing unit.

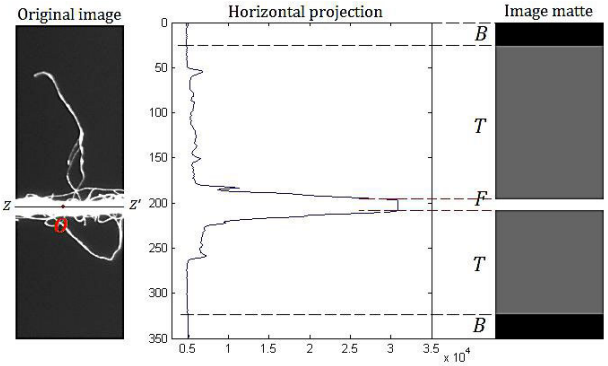

FIGURE 3. Preliminary division of DIPU.

quality. In our work, the image preprocessing mainly includes following two steps, the grey-scale transformation and image filtering. The color images can be converted into grey images by grey-scale transformation easily [29], [29]. The image noises are unavoidable due to the impact of imaging environment and conditions. The image noises can be treated as a kind of indeterminate information. Recently, Neutrosophic Set (NS) has been successfully applied for indeterminate information processing. In this paper, indeterminacy filter is used to process the yarn images. The indeterminacy filter is designed according to the indeterminacy value on the neutrosophic image, while the spatial information is employed to remove the indeterminacy. In this paper, the method proposed in reference [31] is used to preprocess the DIPU. After filtered, the image information of DIPU is enhanced and the edge structure information can be highlighted.

C. DETERMINATION OF THE YARN DIAMETER OF DIPU

According to the diameter image processing unit (DIPU) proposed in Section A above, the yarn diameter at test point O can be calculated. As shown in Fig.3, the left part is a DIPU segmented from the yarn image including the test point O. The diameter of the test point O is expressed by the average diameter of all the points of the axis ZZ′. With this method, the influence of the yarn shape uncertainty on measuring accuracy can be reduced.

1) DIVISION OF DIPU BY PROJECTION ALGORITHM

In this article, the DIPU can be initially divided into definite foreground region F, definite background region B and unknown region T according to projection algorithm which can be found in [7]. Fig.3 shows the preliminary division operation for the DIPU. It was obvious that, the definite foreground region F belongs to the yarn image, and the definite background region B belongs to the image background. Therefore, the next step is to determine which pixel in the unknown region T belongs to the foreground and which belongs to the background.

2) EXTRACTION YARN IMAGE FROM DIPU

In the fact, an image I can be divided into the foreground region F and the background region B by the Poisson matte [32], [33]. They meet the following constraints:

$$I = \alpha F + (1 - \alpha)B, \tag{1}$$

where α is the matting coefficient, and the image I can be linearly represented by image F and image B.

In order to further segment the yarn pattern from the unknown region T, firstly the gradient field of the unknown region is calculated, and then the Poisson's equation can be solved according to the gradient field. The partial derivatives on both sides of equation (2) are taken:

$$\nabla I = (F - B)\nabla\alpha + \alpha\nabla F + (1 - \alpha)\nabla B, \tag{2}$$

Here ∇ is the gradient operator. In this situation, the foreground F and background B are smooth, the actual values of the components $\alpha\nabla F$ and $(1 - \alpha)\nabla B$ in above equation are smaller than the value of component $(\mathrm{F} - \mathrm{B})\nabla\alpha$, then the two components in formula (2) can be omitted. Equation (2) can be translated to follows:

$$\nabla\alpha \approx \frac{1}{F - B}\nabla I, \tag{3}$$

For each pixel i(x,y) in the image, Its intensity is expressed as $\mathrm{I_i}$, and the $\mathrm{F_i}$ and $\mathrm{B_i}$ represent the intensity of the foreground image and the intensity of the background image, respectively. The matting coefficient α can be solved by the following optimization problem:

$$\mathrm{a}^* \approx \arg\min_{\alpha} \iint_{\mathrm{i}\in\mathrm{T}} \left\| \nabla \mathrm{a_i} - \frac{1}{\mathrm{F_i} - \mathrm{B_i}} \nabla \mathrm{_i} \right\|^2 \mathrm{di}, \tag{4}$$

With Dirichlet boundary condition $\alpha|_{\partial \mathrm{T}} = \hat{\alpha}|_{\partial \mathrm{T}}$, (For the pixel i, $\mathrm{N_i}$ means the set of its 4 neighbors.$\partial \mathrm{T} = \{\mathrm{i} \in \mathrm{F} \cup \mathrm{B} | \mathrm{N_i} \cap T \neq \emptyset\}$ is the exterior boundary of T.) then it is can be defined:

$$\hat{\alpha}_i|_{\partial T} = \begin{cases} 1, & i \in F \\ 0, & i \in B, \end{cases} \tag{5}$$

The solution of (4) is the unique solution of the following Poisson equation with Dirichlet boundary conditions (5) [34]:

$$\Delta\alpha = \mathrm{div}(\frac{\nabla I}{F - B}), \tag{6}$$

The equation (6) can be solved by Gauss-Seidel iterative algorithm [35] for each pixel. $(\mathrm{F} - \mathrm{B})$ and $\nabla \mathrm{I}$ are measured in the grayscale channel. F and B are estimated by the points

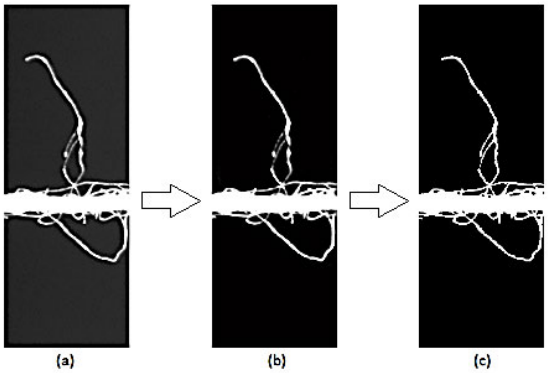

FIGURE 4. Original image. (b) α image. (c) New foreground image.

which were processed and closest to the point i(x,y), in foreground and background, respectively.

The iterative optimization process can be expressed as follows:

a) Initially, for each pixel in unknown region T, F_i and B_i are corresponding the nearest foreground pixels in F and background pixels in B.
b) Then the constructed (F-B) image of each pixel in T is smoothed by a Gaussian filter.
c) After getting the value of (F-B) for each pixel in region T, Poisson equations (6) can be solved and new α for each pixel in region T can be obtained. Then $T_F^+ = \{i \in T | \alpha_i > 0.95, I_i \approx F_i\}$, it means that T_F^+ is mostly foreground. Similarly, $T_B^+ = \{i \in T | \alpha_i < 0.05, I_i \approx B_i\}$, meaning mostly background.
d) Updating the region F and B, $F_{new} = F_{old} \cup T_F^+$ and $B_{new} = B_{old} \cup T_B^+$.
e) Then iterating the above steps (1)∼(4) until change in the matting results(α matrix) is sufficiently small or both T_B^+ and T_F^+ are empty [34].

The new foreground image which is extracted based on Poisson's equation is shown in Figure 4.

3) SEPARATING THE YARN CORE AND HAIRINESS

After the above image processing process, DIPU has been converted into a binary image, in which the pixel with value 0 is the background region and the pixel with value 1 is the yarn region. The next work is to process the new foreground region F to achieve the separation of the yarn core and the hairiness. In this paper, a very simple algorithm to extract the yarn core for each DIPU is proposed by using connectivity of pixels. First of all, it is to ensure the image processing order, in which the pixels above axis ZZ′ are processed from the bottom to the top and the pixels under the axis ZZ′ are processed from the top to the bottom. And then a classifier based on the connectivity is designed. Figure5 shows the schematic diagram of the designed classifier. It can realize the separation of the extracted yarn image pixels into the yarn core and the hairiness. The pixel P is taken as an example to indicate how the classifier works.

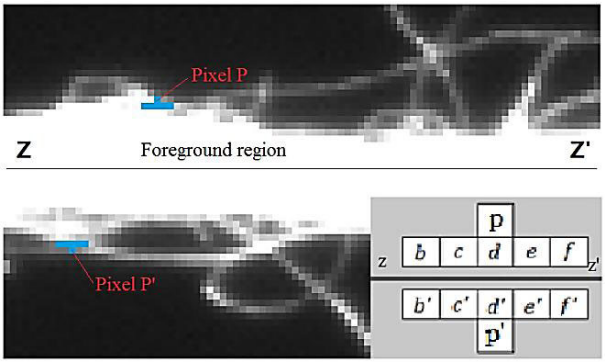

FIGURE 5. Schematic diagram of classifier based on the connectivity.

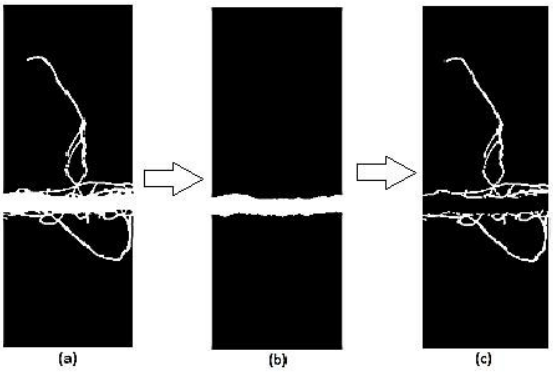

FIGURE 6. (a) New foreground image, (b) yarn core, (c) hairiness.

If the value of pixel P is zero, it belongs to the background. If a pixel is non-zero pixel, the attribution of P pixel according to the value of adjacent pixels is needed to further judge. Only all of the pixels (b, c, d, e and f) are non-zero pixels, the pixel P can be classified as the yarn core. Otherwise, the pixel P is classified as the hairiness. The same way is used to process the pixel P′ under the axis ZZ′. When all the pixels in new foreground image region F are processed by above proposed method, the complete yarn core can be extracted. Figure 6(b) shows the effect of the yarn core extraction.

4) DETERMINATION OF THE YARN DIAMETER

For the selected DIPU, the diameter of test point O is expressed by the average diameter of all the location points of the straight line ZZ′. The line ZZ′ is assumed that contains n pixels, which are expressed by $p_1, p_2, p_3, \ldots p_n$. The diameter through position point p_1 is S_i. Then the diameter of the test point O can be expressed with number of pixels as:

$$R_N = \sum_{i=1}^{n} \frac{S_i}{n} \tag{7}$$

D. CALCULATION METHOD OF YARN HAIRINESS RATE

Yarn hairiness refers to the number of fibers protruding outside the yarn core, which has a direct effect on yarn properties, weaving efficiency, and fabric appearance. As an important indicator, the index of yarn hairiness has been included in

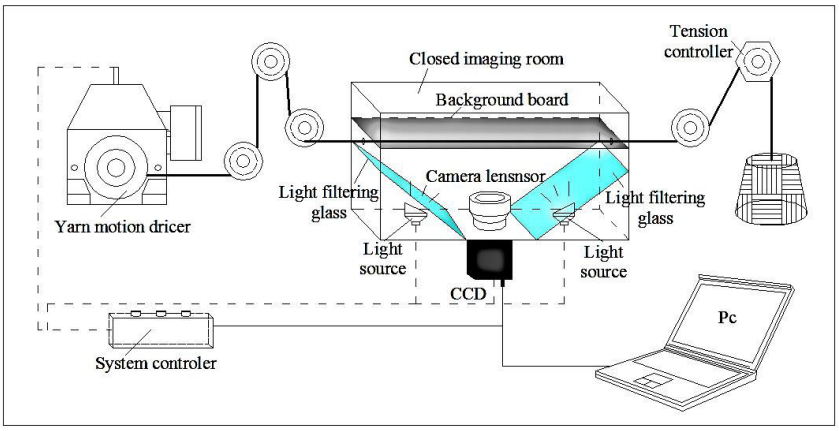

FIGURE 7. System device to detect yarn parameters.

yarn quality requirements [11]. As shown in Figure 4(c), the yarn can be divided into the yarn core and the hairiness. Through above method, the yarn core from the new foreground image based on the connectivity of pixels for each DIPU was extracted. Then the pixels of hairiness also can be obtained by the method of image subtraction. Figure 6(c) shows the extraction of hairiness through the method of image subtraction.

In general, hairiness area index H_A can be defined as the ratio between the total area S_F of single fibers (i.e. looped and protruding) and the total area S_C of core [36]. So in this paper, the hairiness is simplified to be the ratio of the total number of hairiness pixels to the total number of yarn core pixels. The formulas are described as follows [37].

$$H_A = \frac{S_F}{S_C} * 100\% \tag{8}$$

$$S_F = \sum_{i=1}^{M} \sum_{j=1}^{N} f(x_{i,j}) \tag{9}$$

$$S_C = \sum_{i=1}^{M} \sum_{j=1}^{N} c(x_{i,j}) \tag{10}$$

where, f represents pixels of hairiness in the binary image, c represents pixels of the yarn core in the binary image, and M*N represents the size of the image.

E. STATISTICS OF YARN DEFECTS

One of the most important parameters for evaluating yarn quality is yarn defects. The defects of yarn have direct impact on fabric appearance, dyeing absorbability, hand feel, comfort and warmth retention property as well as loom efficiency in the later process. The types of textile yarn defects mainly include thin places, thick places and neps.

As mentioned above, the average diameter of DIPU is used to represent the yarn diameter of the test point, and it is shown as formula (7). If the total number of test points for a yarn test sample is N and the diameter of the test point is expressed as R_i, the average diameter of the yarn sample can be expressed as:

$$d = \sum_{i=1}^{N} R_i / N \tag{11}$$

In order to evaluate the variety of diameter of yarn, the parameter c_i was defined as the rate of change for the diameters of testing points to the average diameter of the yarn sample. According to the value of c_i, all the testing points are classified and the yarn quality can be evaluated.

$$c_i = \frac{R_i}{d} \tag{12}$$

III. SYSTEM DESIGN AND EXPERIMENTS

A. CONFIGURATION OF THE MEASUREMENT SYSTEM

In this article, a corresponding measuring system is designed to achieve the measurement of yarn diameter, hairiness and defects. In the designed system, a closed room is used as the image-capturing platform to shield the disturbance of the stray light. A milky white diffused glass is adopted to eliminate reflected light and shadow. In addition, yarn motion driver and tension controller are used to obtain better simulation. Fig.7 shows the integrated structure of this system.

Yarn image-capturing system is mainly composed by three parts: the first part is imaging system, including CCD image sensor, camera lens and light source, among which the CCD image sensor is used to collect the sequence of the yarn image. The system chooses imaging lens with large depth of field to ensure that hairiness of different position can be clearly imaged. The images were acquired by a SONY Zoom Lens C with a focal length of 12.5 to 75 mm connected to a digital charge-coupled device (CCD) camera (Basler acA2040-180km/kc, pixel size 5.5μm, resolution of 2048$\times$2048 pixels, sampling rate 180 fps), and a personal computer with an image processor.

In order to minimize the influence of outside, the half-box housing is used in the closed fixed imaging room. The yarn to be tested will pass through the imaging box, and one end of the yarn is connected to the yarn motion driver while the other

TABLE 1. Specifications of test yarns.

Sample No	Linear mass (Tex)	Material description	Spinning system	Twist (turns/m)	Sample size
1	53.01	Combed cotton yarn	Ring spinning	848	10
2	16.62	Combed cotton yarn	Rotor spinning	812	10
3	16.41	Combed wool yarn	Ring spinning	452	10
4	16.22	Combed wool yarn	Ring spinning	486	10
5	16.12	Polyester filament air-textured yarn	Rotor spinning	/	10
6	16.73	Nylon filament air-textured yarn	Rotor spinning	/	10
7	16.73	Polyester filament false-twist textured yarn	Rotor spinning	/	10
8	16.64	Nylon filament false-twist textured yarn	Rotor spinning	/	10

end of the yarn is connected to the tension controller through wire devices. The second part is control system, including yarn tension controller, wire devices and yarn motion driver. The cross-section of the yarn will be affected by the tension, so the yarn tension needs to be kept constant during the process of measurement. The third part is computer and image processing software. After the parameters were set, the yarn tension and motion speed can be controlled precisely, and the automatic measurement for the yarn diameter and hairiness is realized. Finally, in the designed on-line detection system, the yarn moves at a speed of 20m/min, and the camera sampling rate is 30 frames per second.

B. TESTING SAMPLE MATERIAL

In experiment, eight types of yarn which are produced by different manufacturers are used as test objects, and the size of each type of samples is 10. Table 1 shows the parameters of the yarns, which are consist of cotton, wool, nylon or polyester, and spun by ring or rotor machines.

C. EXPERIMENT

1) MEASUREMENT OF YARN DIAMETER AND HAIRINESS

Using the above method, the yarn measurement experiment is carried out. In order to ensure the stability of the measurement system and the reproducibility of the measurement results, the measurement system is firstly calibrated by the precise calibration ruler. According to the two grade atmosphere standard of GB6529, namely temperature is 20±2° and humidity is 65%+2%. The testing parameters are set as follows: the detection speed is 20m/min, yarn tension is 50mN, and the effective testing length of each sample is 1000 meters. In order to analyze the influence of parameter δ on the test results, two different parameters $\delta = 2$mm and $\delta = 5$mm are used to test the same yarn samples respectively. Moreover, the experimental results presented in this paper are compared with the results coming from the capacitive evenness method.

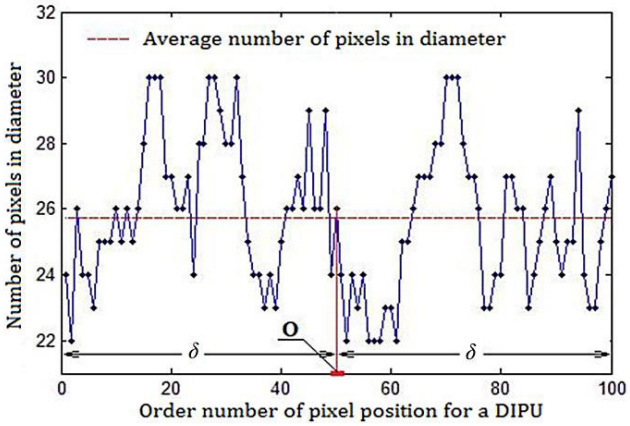

FIGURE 8. Number of pixels occupied by yarn diameter at different positions.

As described above, the average diameter of all pixel points in DIPU with 2δ length was taken as the diameter of the test point O. Figure.8 shows one of test results of a DIPU corresponding to a yarn test point O, in which δ is 5mm. It can be seen from Figure.8 that the number of position points is 100 within the neighborhood of ($-\delta$, δ) and the average diameter is 25.75 pixel width which represents the diameter of the test point O.

To test the effectiveness of our proposed method, the diameters of eight groups of samples were measured by the proposed method and capacitive evenness tester called the Uster Tester under the same condition, and the diameter and hairiness rate for yarn samples were obtained. Table 2 shows the test results of 10 samples in type 1 which was produced in different batches. In this experiment, each sample was tested separately with different methods and different parameters δ.

In order to compare and observe change rules between the measured data from two methods more intuitively, the experimental data obtained is processed, and the result is shown in Figure 9 in which the parameter δ is set to 5 mm.

TABLE 2. Measuring result on diameter and hairiness from sample type 1.

Sample number	The proposed method				Uster tester
	δ=2mm		δ=5mm		
	Average value of yarn diameter/mm	Estimation of hairiness rate/%	Average value of yarn diameter/mm	Estimation of hairiness rate/%	Yarn diameter/mm
1	0.293	17.6	0.272	16.1	0.294
2	0.272	16.1	0.261	13.8	0.281
3	0.324	18.4	0.282	17.2	0.331
4	0.324	16.2	0.261	14.0	0.332
5	0.240	11.5	0.240	12.4	0.248
6	0.251	13.2	0.272	14.3	0.277
7	0.240	11.5	0.251	12.6	0.256
8	0.282	15.6	0.272	13.8	0.301
9	0.303	17.1	0.293	16.8	0.311
10	0.314	16.7	0.282	15.6	0.315
Average value of 10 samples	0.284	15.4	0.269	14.7	0.295

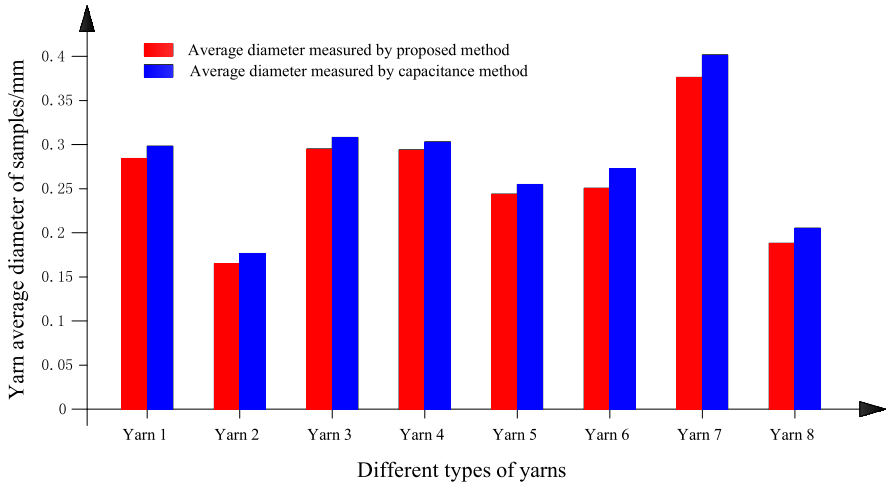

FIGURE 9. Measuring result on diameter from eight types of yarns.

2) DETECTION OF YARN DEFECTS

Because yarn defect is an important index to characterize yarn evenness, the analysis of yarn defects is significant to the evaluation of yarn quality. In this paper, an experiment to detect yarn defects was carried out by the designed detection system, and the setting of environmental parameters is described as section 3.3.1.

Firstly, the system parameters are set according to the requirements of the test. In this paper, the yarn defects are classified based on the value of dimensionless parameter c_i, the sample points with c_i value greater than 2.8 are defined as neps. The thick places show an increase in the diameter, normally the c_i value range from 2.8 to 1.25. The thin places show a decrease of diameter, normally the c_i value range from 0 to 0.75 [38], [39].The length of yarn sample is 1000 meters. The axial distance of sampling interval is 5mm, and the parameter δ is set to 2mm. Finally, the actual yarn defects are classified according to the digital interval. The experimental data of yarn defects is shown in Tables 3 and Figure.11.

D. ANALYSIS AND DISCUSSION

1) DIAMETER FROM TWO DIFFERENT METHODS

As shown in Table 2 and Figure.9, the results tested by two methods are very close. The yarn diameter measured by the capacitance method is obviously larger than that measured by the method proposed in this paper. The distinction of

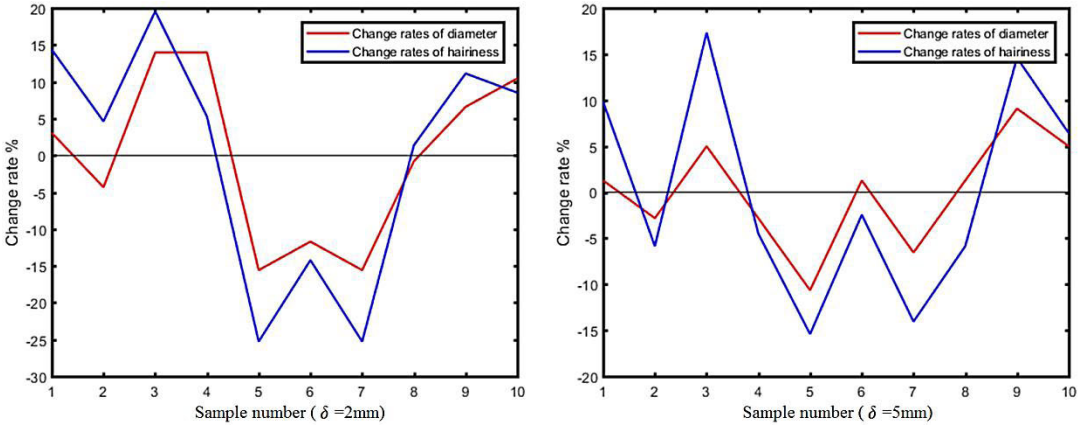

FIGURE 10. Variation on diameter and hairiness of 10 samples in sample type 1.

TABLE 3. Measuring result of defects by proposed method and capacitance method.

Type of yarn	Thick places (/km)				Thin places (/km)				Neps (/km)	
	Machine vision method		Uster tester		Machine vision method		Uster tester		Machine vision method	Uster tester
	c_i = 2.8-1.5	c_i = 1.5-1.25	c_i = 2.8-1.5	c_i = 1.5-1.25	c_i = 0.75-0.5	c_i = 0.5-0	c_i = 0.75-0.5	c_i = 0.5-0	c_i>2.8	c_i>2.8
1	815	951	897	1047	2088	5	1879	2	0	0
2	829	942	981	1036	1912	6	1720	3	1	1
3	668	2421	735	2711	2310	52	2079	31	0	0
4	594	2528	653	2730	2145	54	2359	27	2	3
5	619	2893	681	3182	2456	6	2112	2	1	2
6	797	3298	877	3628	2771	3	2980	1	1	1
7	299	5549	329	6049	6669	8	5531	3	0	0
8	146	4132	159	4525	4574	68	3888	35	0	1

the measurement results is caused by the different of testing principles. As we all know, the principle of Uster Tester is to use capacitance conversion methods to calculate the yarn diameter through empirical relationships. This means that this method is more susceptible to hairiness and moisture. The detection method proposed in this paper is based on visual imaging, which can effectively avoid the influence of changes in yarn hairiness and moisture. Therefore, the method based on machine vision has better accuracy and robustness for yarn diameter detection.

2) VARIATION OF DIAMETER WITH HAIRINESS

Figure.10 shows the variation of diameter with the hairiness rate of sample type 1, in which the parameter δ is set to 2mm and 5mm respectively. When the parameter δ is set to 2mm, it can be seen that the range of change rate in diameter is $[-15.58\%, +13.96\%]$, and the range of change rate in hairiness is $[-25.28\%, +19.56\%]$. When the parameter δ is set to 5mm, the range of change rate in diameter is [-10.65%, +9.08%], and the range of change rate for corresponding hairiness varies from $[-15.42\%, +17.33\%]$. From the experimental data of the two charts above, it can be seen that large changes in hairiness will aggravate the irregularity of the yarn core.

3) EFFECT OF PARAMETER δ

Parameter δ is the valid distance on the two endpoints of test point O in axial direction, and it is an important parameter that determines the size of DIPU segmented from captured image. According to the acquired test results, it can be calculated that when $\delta = 2$mm, the variation coefficient CV_2 for average diameter is 11.52%, the absolute mean deviation U_2 is 9.60%, the maximum value for coefficient range $Pmax_2$ is 29.55%. When $\delta = 5$mm, the variation coefficient CV_5 for average diameter is 5.86% and the absolute mean deviation U_5 is 4.570% and the maximum value for coefficient range $Pmax_5$ is 19.73%. While $CV_2 > CV_5$, $U_2 > U_5$, it can be concluded that the larger δ is, the more points in the neighborhood will

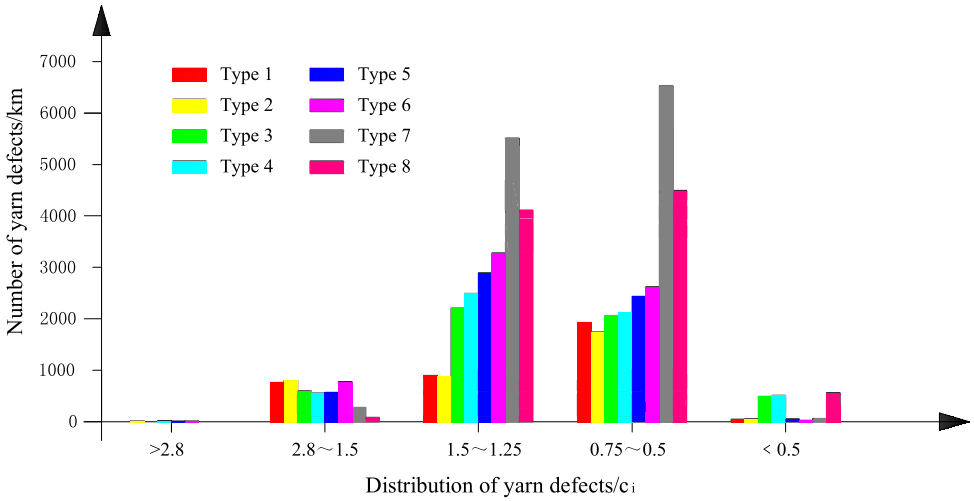

FIGURE 11. Measuring result of yarn defects by proposed method.

be included in the calculation, and the random error will be smaller. Similarly, the smaller δ is, the fewer points included, and the random errors will be greater.

4) DEFECTS OF TWO DIFFERENT METHODS

Figure.11 is derived from Table 3 which shows the detecting results on yarn from different type yarns by the proposed method. As it can be seen from Figure.11, the filament false-twist textured yarn and air-textured yarn have more yarn defects and more frequent changes than combed cotton/wool yarn. This is why the combed cotton/wool yarn can give us a more natural and beautiful visual appearance. The above conclusion is not only consistent with the subjective visual evaluation, but also proves that the yarn quality can be evaluated objectively by means of experiments. It shows that the proposed method is feasible to judge the yarn diameter change and appearance.

IV. CONCLUSION

Based on image processing and machine vision, the paper proposed a new method to evaluate yarn quality by detecting the diameter, hairiness and faults. Experiments are carried out and the detection results are analyzed. Compared with the existing methods, the proposed method has the following advantages.

First of all, because the yarn shape is changeable, the diameters measured at different points are different. In this paper, the diameter of yarn test point is expressed by the average value of all position points in DIPU, which can effectively avoid the influence of random factors on the test results. Obviously, the proposed method can meet different testing requirements by choosing different parameters for DIPU and achieve yarn quality evaluation flexibly.

Secondly, due to the evaluation of yarn quality based on the method of sequential sampling points, the yarn core and the hairiness of DIPU selected by testing points can be separated accurately by image processing algorithm. Therefore, it is easy to obtain the statistical information of the yarn diameter and the law that the yarn diameter changes with the test position of the yarn sample. This will help to evaluate yarn quality reliably.

Finally, the proposed method realized not only a flexible detection of yarn diameter, but also the measurement of yarn hairiness and defects. In addition, the proposed method and corresponding detection system make it easier to automate and industrialize online yarn detection.

REFERENCES

[1] S. Roy, A. Sengupta, and S. Sengupta, "Performance study of optical sensor for parameterization of staple yarn," *Measurement*, vol. 109, pp. 394–407, Oct. 2017.
[2] M. Datta Roy, R. Chattopadhyay, and S. K. Sinha, "Wicking performance of profiled fibre part B: Assessment of fabric," *J. Inst. Eng. India E*, vol. 99, no. 1, pp. 1–8, Jun. 2018.
[3] N. H. Maruf, "Comparative study of conventional carded and compact ring Spun Yarn," *Res. J. Sci. IT Manage.*, vol. 5, no. 5, pp. 1–4, 2016.
[4] V. Ghorbani, M. Vadood, and M. S. Johari, "Prediction of polyester/cotton blended rotor-spun yams hairiness based on the machine parameters," *J. Textile Res.*, vol. 41, no. 1, pp. 19–25, 2016.
[5] Y. Chen, B. Xu, J. Wen, J. Gong, T. Hua, C.-W. Kan, and J. Deng, "Design of novel wearable, stretchable, and waterproof cable-type supercapacitors based on high-performance nickel cobalt sulfide-coated etching-annealed yarn electrodes," *Small*, vol. 14, no. 21, May 2018, Art. no. 1704373.
[6] G. Redlich, E. Obersztyn, and M. Olejnik, "New textiles designed for anti-radar camouflage," *Fibres Textiles Eastern Eur.*, vol. 103, no. 1, pp. 34–42, 2014.
[7] P. Zhong, Z. Kang, S. Han, R. Hu, J. Pang, X. Zhang, and F. Huang, "Evaluation method for yarn diameter unevenness based on image sequence processing," *Textile Res. J.*, vol. 85, no. 4, pp. 369–379, Mar. 2015.
[8] Y. Sun, N. Zhang, and Y. Wu, "Tracking measurement of yarn hairiness skeleton and length," *J. Textile Res.*, vol. 38, no. 8, pp. 32–38, 2017.
[9] Y. Sun, Z. Li, R. Pan, J. Zhou, and W. Gao, "Measurement of long yarn hair based on hairiness segmentation and hairiness tracking," *J. Textile Inst.*, vol. 108, no. 7, pp. 1271–1279, 2017.
[10] V. K. Yadav, S. M. Ishtiaque, S. D. Joshi, and J. K. Chatterjee, "Diametric unevenness and fault classification of yarn using newly developed diametric fault system," *Fibers Polym.*, vol. 18, no. 10, pp. 2018–2033, Oct. 2017.
[11] R. Wang, J. Zhou, L. Yu, and B. Xu, "Fusing multifocus images for yarn hairiness measurement," *Opt. Eng.*, vol. 53, no. 12, pp. 123101.1–123101.7, Dec. 2014.
[12] J. Wang, B. Xu, Z. Li, W. Gao, and L. Wang, "Depth recovery of hairy fibers for precise yarn hairiness measurement," *Appl. Opt.*, vol. 57, no. 24, p. 7021, Aug. 2018.

[13] V. Carvalho, P. Cardoso, M. Belsley, R. Vasconcelos, and F. Soares, "Yarn diameter measurements using coherent optical signal processing," *IEEE Sensors J.*, vol. 8, no. 11, pp. 1785–1793, Nov. 2008.

[14] G. Q. Zhou, W. Xi, and R. W. Yuan, "Algorithm of yarn core diameter extraction based on linear array CCD," *J. Tianjin Polytech. Univ.*, vol. 2, pp. 35–39, Apr. 2016.

[15] L. Cheng, X. Jiang, and R. Yuan, "Measuring method of yarn diameter based on line array charge-coupled device," *J. Textile Res.*, vol. 36, no. 6, pp. 124–128, 2015.

[16] S. M. Ishtiaque and A. Das, "A new approach of prediction of yarn diameter," *Fibers Polym*, vol. 14, no. 5, pp. 838–843, May 2013.

[17] R. W. Yuan, X. M. Jiang, and G. Q. Zhou, "Measuring method of yarn diameter and hairiness based on linear array," *J. Textile Res.*, vol. 34, no. 8, pp. 132–137, 2013.

[18] M. Tàpias, M. Ralló, and J. Escofet, "Automatic measurements of partial cover factors and yarn diameters in fabrics using image processing," *Textile Res. J.*, vol. 81, no. 2, pp. 173–186, Jan. 2011.

[19] A. Fabijańska and L. Jackowska-Strumiłło, "Image processing and analysis algorithms for yarn hairiness determination," *Mach. Vis. Appl.*, vol. 23, no. 3, pp. 527–540, May 2012.

[20] J. Li, B. Zuo, C. Wang, and W. Tu, "A direct measurement method of yarn evenness based on machine vision," *J. Eng. Fibers Fabrics*, vol. 10, no. 4, Dec. 2015, Art. no. 155892501501000.

[21] Z. Li, N. Xiong, J. Wang, R. Pan, W. Gao, and N. Zhang, "An intelligent computer method for automatic mosaic of sequential slub yarn images based on image processing," *Textile Res. J.*, vol. 88, no. 24, pp. 2854–2866, Dec. 2018.

[22] Z. Li, R. Pan, J. Zhang, B. Li, W. Gao, and W. Bao, "Measuring the unevenness of yarn apparent diameter from yarn sequence images," *Meas. Sci. Technol.*, vol. 27, no. 1, Jan. 2016, Art. no. 015404.

[23] Y. A. Ozkaya, "Digital image processing and illumination techniques for yarn characterization," *J. Electron. Imaging*, vol. 14, no. 2, Apr. 2005, Art. no. 023001.

[24] X. Mou, Y. Cai, X. Zhou, and G. Chen, "On-line yarn cone defects detection system based on machine vision," *J. Textile Res.*, vol. 39, no. 1, pp. 139–145, 2018.

[25] N. Gonçalves, V. Carvalho, M. Belsley, R. M. Vasconcelos, F. O. Soares, and J. Machado, "Yarn features extraction using image processing and computer vision—A study with cotton and polyester yarns," *Measurement*, vol. 68, pp. 1–15, May 2015.

[26] D. Çukul and Y. Beceren, "Yarn hairiness and the effect of surface characteristics of the ring traveller," *Textile Res. J.*, vol. 86, no. 15, pp. 1668–1674, Sep. 2016.

[27] W. Wang, B. Xin, D. Na, J. Li, and N. Liu, "Identification and application of yarn hairiness using adaptive threshold method under single vision," *Textile Res. J.*, vol. 40, no. 5, pp. 150–156, 2019.

[28] J. Jing, M. Huang, P. Li, and X. Ning, "Automatic measurement of yarn hairiness based on the improved MRMRF segmentation algorithm," *J. Textile Inst.*, vol. 109, no. 6, pp. 740–749, Jun. 2018.

[29] Y. Guo and H. Cheng, "New neutrosophic approach to image segmentation," *Pattern Recognit.*, vol. 42, no. 5, pp. 587–595, May 2009.

[30] P. Zhong, Y. Shi, X. Chen, Q. Tan, and C. Zhang, "Research on digital intelligent recognition method of the weave pattern of fabric based on the redundant information," *Fibers Polym*, vol. 14, no. 11, pp. 1919–1926, Nov. 2013.

[31] Y. Guo, R. Xia, A. Şengür, and K. Polat, "A novel image segmentation approach based on neutrosophic c-means clustering and indeterminacy filtering," *Neural Comput. Appl.*, vol. 28, no. 10, pp. 3009–3019, Oct. 2017.

[32] S. Renukalatha and K. V. Suresh, "Segmentation of noisy PET images using Bayesian matting," in *Proc. Int. Conf. Contemp. Comput. Inform. (IC3I)*, Nov. 2014, pp. 1160–1165.

[33] X. Yan, Z. Hao, and H. Huang, "Alpha matting with image pixel correlation," *Int. J. Mach. Learn. Cyber.*, vol. 9, no. 4, pp. 621–627, Apr. 2018.

[34] J. Sun, J. Jia, C.-K. Tang, and H.-Y. Shum, "Poisson matting," *ACM Trans. Graph.*, vol. 23, no. 3, p. 315, Aug. 2004.

[35] P. Pérez, M. Gangnet, and A. Blake, "Poisson image editing," *ACM Trans. Graph.*, vol. 22, no. 3, p. 313, Jul. 2003.

[36] A. Guha, C. Amarnath, S. Pateria, and R. Mittal, "Measurement of yarn hairiness by digital image processing," *J. Textile Inst.*, vol. 101, no. 3, pp. 214–222, Feb. 2010.

[37] W. Wang, B. Xin, N. Deng, J. Li, and N. Liu, "Single vision based identification of yarn hairiness using adaptive threshold and image enhancement method," *Measurement*, vol. 128, pp. 220–230, Nov. 2018.

[38] F. Pereira, V. Carvalho, F. O. Soares, R. M. Vasconcelos, and J. Machado, "Computer vision techniques for detecting yarn defects," *Appl. Comput. Vis. Fashion Textiles*, vol. 22, pp. 123–145, Jan. 2018.

[39] M. H. J. Van Der Sluijs and L. Hunter, "A review on the formation, causes, measurement, implications and reduction of neps during cotton processing," *Textile Progr.*, vol. 48, no. 4, pp. 221–323, Oct. 2016.

ZHISONG LI received the bachelor's and master's degrees from the Henan University of Science and Technology, Henan, China, in June 2013. He is currently pursuing the Ph.D. degree with Donghua University, Shanghai, China. He engaged in the research of optical sensors and optical metrology.

PING ZHONG received the bachelor's degree in computer science from Jilin University, Jilin, China, in June 1996, and the master's and Ph.D. degrees in optical engineering from the Chinese Academy of Sciences, Jilin, in June 2004. He is currently a Professor with Donhua University, Shanghai, China. His research fields include optical metrology, image processing, and optical sensors.

XIN TANG received the bachelor's degree in electronic and information engineering from the Shanghai University of Engineering Science. He is currently pursuing the master's degree in optical engineering with Donghua University. He engaged in the research of optical metrology, image processing, and optical sensors.

YU CHEN is currently pursuing the bachelor's degree in optical engineering with Donghua University. His research fields include optical metrology and optical sensors.

SHU SU received the bachelor's degree in optoelectronic technology and science from Donghua University, where he is currently pursuing the master's degree in optical engineering. He engaged in the research of optical metrology, image processing, and optical sensors.

TIANBAO ZHAI received the bachelor's degree in optoelectronic technology and science from Donghua University, where he is currently pursuing the master's degree in optical engineering. He engaged in the research of optical metrology, image processing, and optical sensors.